ORIGINAL ARTICLE

Analysis of Magnetic Assisted Assembly of Meso-Scale Parts

Hong-Hua Ko and Dung-An Wang*

Graduate Institute of Precision Engineering, National Chung Hsing University, Taiwan

(**Received** 1 September 2013; **Accepted** 4 October 2013; **Published on line** 1 June 2014)

*Corresponding author: daw@nchu.edu.tw

DOI: 10.5875/ausmt.v4i2.278

Abstract: This paper presents an analysis of the self-assembly of millimeter-sized, rectangular-shaped parts floating on a molten solder-air interface under a rotating external magnetic field. For part at the millimeter scale, gravitational effects may not be negligible compared to interfacial surface energy, resulting in a non-spontaneous self-assembly process. A rotating magnetic field produces a torque which rotates the magnetized parts into their specific in-plane orientations, and are then fixed in these orientations by the surface tension of the molten solder. A theoretical model for estimating the magnetic torque is developed. Experiments are carried out on glass substrates with patterned copper foil. Rectangular binding sites are the only hydrophilic areas on the substrate. By a simple coating process, molten solder wets only the binding sites on the substrate. Parts with orientation angles up to 90° can be rotated and translated to align with the binding sites by the magnetic torque and surface tension.

Keywords: Magnetic; molten solder; self-assembly; surface tension

Introduction

Different strategies are used to assemble meso and micro scale components in complex heterogeneous integrated systems, including conventional pick and place robotic assembly [1-3], microstructure transfer between aligned wafers [4, 5], and dynamic self-assembly [6]. Robotic assembly is a serial process and can be subject to adhesion forces resulting from the handling and positioning of micro/nano components. Wafer-level transfer is an inherently two-dimensional fabrication method and cannot generate truly three-dimensional structures [7]. Self-assembly is generally a batch process in which micro-fabricated components are automatically integrated and constructed as functional units. Gracias et al. [8] demonstrated the self-assembly of sophisticated, three-dimensional networks of millimeter-scale polyhedra, with surfaces patterned with solder dots, wires, and light-emitting diodes, in a hot, isodense, aqueous KBr solution.

For the final assembled structure to be functional, part assembly requires a method to maintain the mechanical connection of the final structure and electrical connection between components. Different methods can be used to establish the electrical connection between parts for wafer to wafer bonding, including the use of solders applied by electroplating, screen printing or sputtering [9]. However, the electrical contacts produced by electroplated solders suffer from poor mechanical properties [10]. Polymer interconnections show great promise as conducting materials in a wide range of application areas due to their tolerance of mechanical stress, ease of processing and chemical tenability [11]. Nevertheless, these polymers exhibit high electrical resistivity, their contact area may be limited to asperities and they may be unable to withstand high-temperature processing and operation at the molecular level [7, 12]. Soldering processes for assembling parts to one another or to a substrate provide excellent electrical, thermal, and mechanical properties. In soldering processes, microparts are aligned to binding sites via a layer of molten solder due to total energy minimization.

Surface tension is the driving force for the self-assembly technique using molten solder, especially in fluid environments [13, 14]. For micro/nano scale parts, the self-assembly process can be driven by surface tension with fluid agitation [13, 15] or simply through minimization of interfacial free energy [13]. When assembling millimeter-sized parts in an air environment, a source of external agitation may be needed to assist the assembly process. With proper agitation in the fluid environment, millimeter-sized parts can settle into the required orientations with the local minimum surface energy [10, 16]. As noted by Leong et al. [17], surface forces scale favorably with deceasing part sizes, and self assembly driven by surface tension has the potential for the assembly of micro- and nano-scale parts. As the weight of millimeter-scale parts increases, gravitational forces begin to dominate, thus potentially rendering the self-assembly nonspontaneous. Therefore, assembly of large, millimeter-sized parts may require a combination of surface tension and other driving forces.

Methods of assembling parts using molten solder or liquid have been developed with different driving mechanisms [15, 16, 18-23]. By minimizing the surface energy of molten solder balls, Harsh et al. [19] demonstrated an assembly of a hinged plate through controlling the solder volume. Ye et al. [22] used a magnetic field to integrate nanowires with a solder-padded substrate. Gagler et al. [24] assembled two-dimensional structures to from three-dimensional solids by a combination of magnetic and surface tension forces in water. Morris and Parviz [15] assembled circular and square microparts to binding sites on a silicon template with a surface treatment and a reflow process in a fluid environment. Fang et al. [18] demonstrated the orbital shaking-assisted self assembly of square PZT parts in an air environment.

This paper presents analyses of an on-substrate self-assembly of millimeter-sized, magnetized, rectangular parts using molten solder. A rotating magnet is used to assist the assembly and ensure the accurate placement of parts in an air environment. Theoretical analysis of magnetic torques is carried out to predict the driving capability of the rotating magnet. Experiments demonstrate the parallel self-assembly of multiple parts.

Hong-Hua Ko received the M.S. degree in Graduate Institute of Precision Engineering, National Chung Hsing University, Taiwan, ROC., in 2010.

Dung-An Wang received the Ph.D. degree in mechanical engineering from the University of Michigan at Ann Arbor, in 2004. He is currently a Professor in the Graduate Institute of Precision Engineering, National Chung Hsing University, Taiwan, ROC. His research interests include micromachined sensors and actuators, piezoelectric actuators, microassembly and compliant mechanisms.

Magnetic Assisted Self-Assembly

A rotating magnetic field can provide a torque for the self-assembly of millimeter-sized, magnetized parts. Doing so in an air environment may require a source of external agitation to assist the assembly process as the size of the parts is scaled up. A rotating magnet provides agitation to overcome the friction or sticking force between the parts and binding site. Figure 1 illustrates the operation steps of the self-assembly process. Figure 1(a) shows a binding site of a substrate and a misaligned part resting on the binding site. Before the part is placed, a layer of molten solder is applied on the binding site. A permanent magnet is placed at a distance D below the substrate. The part sinks into the molten solder during experiments, and cannot be rotated by the magnet. Another permanent magnet is placed at a distance Δ above the substrate to cause the part to rise into the air against gravity. When the magnet below the substrate is rotated with an angular velocity Ω, a magnetic torque is applied to the part to align it with the binding site as shown in Figure 1(b). The part can be rendered ferromagnetic by electroplating a nickel layer at its bottom surface.

In principle, a threshold value exists for the angular velocity of the rotating magnet for successful part assembly. Based on experimental observations, for the successful runs, the parts are rotated quickly and swung into perfect alignment. The alignment of the parts may be achieved by the angular momentum provided by the rotating magnet to overcome the gravitational, frictional and sticking effects due to contact with the solder.

Model

An analytical model is developed to estimate the torque needed to align the part with the binding site. As shown in Figure 1(a), a torque T is generated by the magnet to align a part with a binding site. A restoring torque τ introduced by the molten solder due to surface energy minimization is also shown in the figure. The part can be respectively rotated and retarded by the magnetic torque T and the restoring torque τ. To successfully align the part ith the binding site, the maximum magnitude of T should be greater than the maximum magnitude of τ for the part's various orientations. Also, the maximum magnitude of T should be less than the magnitude of τ at the aligned orientation to assure that the restoring torque keeps the aligned part in perfect alignment while the magnetic torque is applied.

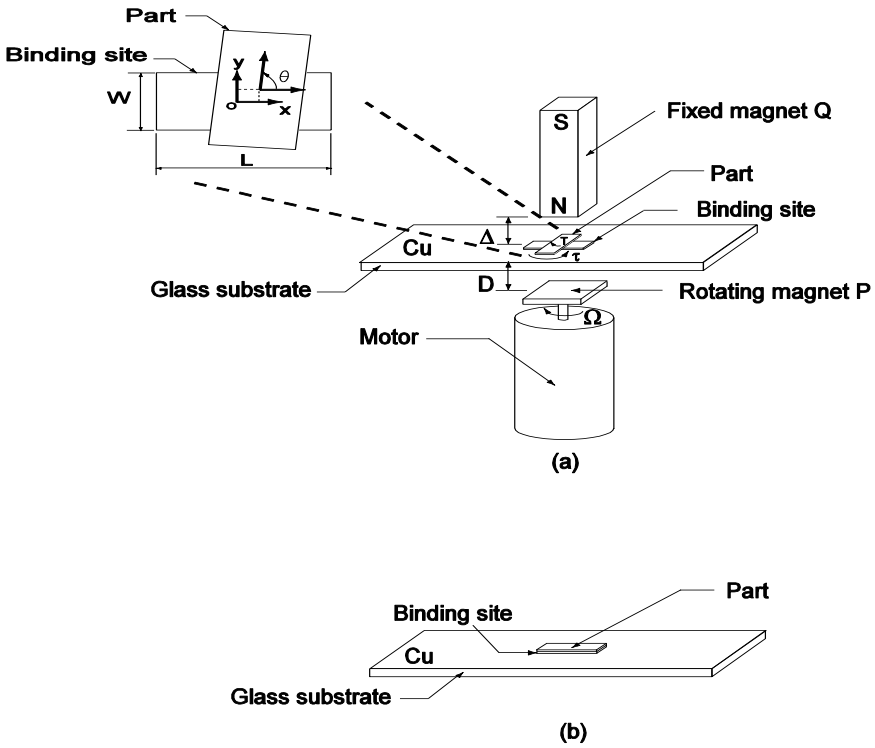

Figure 1. Two-step operation of the self-assembly of a part. (a) A rectangular magnet rotates at angular velocity of Ω below a substrate. (b) The resulting alignment of the part.

Estimation of the Magnetic Torque

Consider a rectangular magnet P below the part and a rectangular magnet Q above the part as shown in Figure 2(a). A Cartesian coordinate system with its origin located at the center of the magnet P is also shown in the figure. The magnet P with length L_P, width W_P and height H_P has a magnetization vector M_P along the x axis. The z axis coincides with the axis of rotation of the magnet P. The magnet Q with length L_Q, width W_Q and height H_Q has a magnetization vector M_Q along the z axis. Using the Biot-Savart law and the equivalent current density method [25], the magnetic flux density B_P and B_Q of the magnet P and Q can respectively be expressed as

$$B_P(x,y,z)=\frac{\mu_0 M_P}{4\pi}\int_{-L/2}^{L/2}\oint_{C_P'}\frac{d\vec{l}_P'\times\vec{R}_P}{R_P^3}dx', \tag{1}$$

$$B_Q(x,y,z)=\frac{\mu_0 M_Q}{4\pi}\int_{\frac{H_P}{2}+D+\Delta}^{\frac{H_P}{2}+D+\Delta+L_Q}\oint_{C_Q'}\frac{d\vec{l}_Q'\times\vec{R}_Q}{R_Q^3}dz', \tag{2}$$

where μ_0 is the permeability of free space, the position vectors $\vec{R}_P$ and $\vec{R}_Q$ are respectively measured from $d\vec{l}_P'$ and $d\vec{l}_Q'$ at a source point (x',y',z') to a field point (x,y,z) for the magnets P and Q, as illustrated in Figure 2(b). C_P' and C_Q' are respectively the closed paths enclosing the differential sections of the magnets P and Q.

It is assumed that the part's magnetization direction of the part is the same as that of its long axis and the hysteretic effects are negligible; these assumptions are often valid for soft-magnetic materials [26]. The internal field H_i is a function of the applied field H and a demagnetizing field H_d as

$$H_i=H+H_d, \tag{3}$$

where H is evaluated by B/μ_0. The demagnetization field can be expressed as

$$H_d=-NH, \tag{4}$$

where N is a tensorial demagnetization factor. Assuming the part's magnetization direction is the same as its long axis direction, i.e. x axis, the xx component of the demagnetization factor is given by [27]

$$\begin{aligned}N_{xx}=(1/4\pi)\{&\cot^{-1}f(x,y,z)+\cot^{-1}f(-x,y,z)\\&+\cot^{-1}f(x,-y,z)+\cot^{-1}f(x,y,-z)\\&+\cot^{-1}f(-x,-y,z)+\cot^{-1}f(-x,y,-z)\\&+\cot^{-1}f(-x,y,-z)+\cot^{-1}f(-x,-y,-z)\}\end{aligned}, \tag{5}$$

where

$$f(x,y,z)=\frac{\left[\left(\frac{L_{ni}}{2}-x\right)^2+\left(\frac{W_{ni}}{2}-y\right)^2+\left(\frac{H_{ni}}{2}-z\right)^2\right]^{\frac{1}{2}}\left(\frac{L_{ni}}{2}-x\right)}{\left(\frac{W_{ni}}{2}-y\right)\left(\frac{H_{ni}}{2}-z\right)}, \tag{6}$$

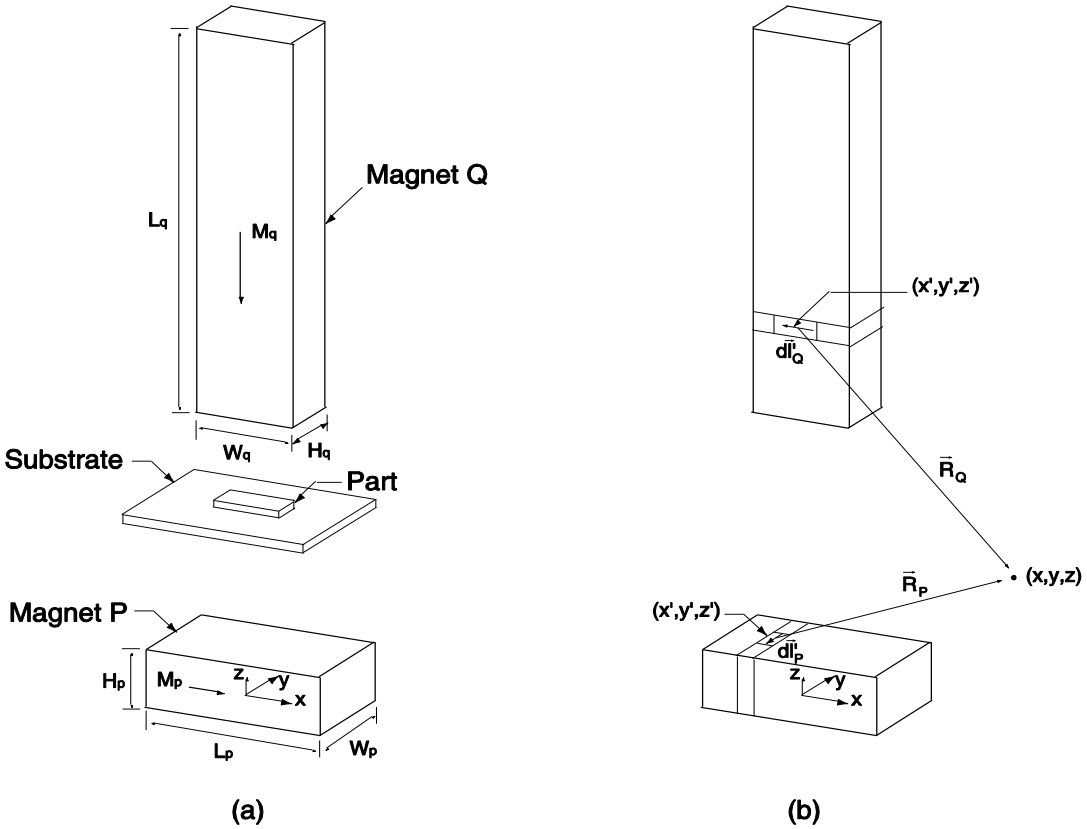

Figure 2. (a) Schematic of a part, magnet P and magnet Q. (b) Position vectors and system of coordinates used in the current-sheet calculations of the magnetic field.

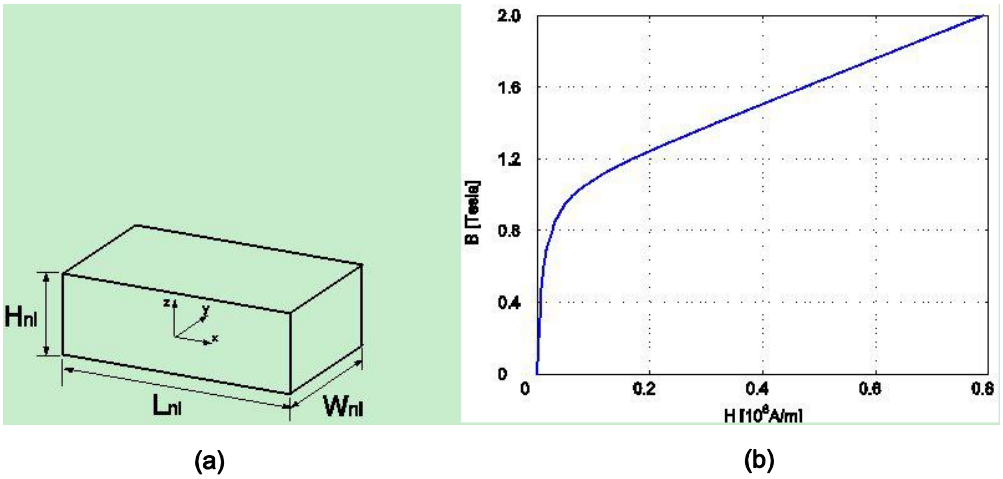

Figure 3. (a) Schematic of a part and its coordinate system. (b) B as a function of H of an electroformed nickel.

Figure 3(a) presents a schematic of a part and its coordinate system. The origin of the coordinate system used for (5) and (6) coincides with the center of the part and the axes are aligned with the principal axes of the part. The length, width and height of the part are respectively denoted as L_{ni}, W_{ni} and H_{ni}. The magnetic torque T acting on the part is found by the principle of virtual displacement

$$\mathrm{T} = \frac{\partial W_m}{\partial \theta}, \tag{7}$$

where W_m is the magnetic energy stored in the part and is given as

$$W_m = \frac{1}{2}\int_{V'} H_i \cdot B_i dv', \tag{8}$$

where V' is the part's volume of the part and B_i is its internal flux density.

Estimation of the Restoring Torque

For systems exhibiting a simple geometry, analytical models can be used to determine surface force

[28]. To estimate the surface force of systems with complex shapes, numerical simulations should be used to account for three-dimensional geometry and nonlinear effects. In this investigation, the Surface Evolver software package [29, 30] is used to obtain the minimal energy surface and to estimate the total energy during the assembly process. The total energy arises from surface tension and gravitational energy. The restoring torque τ is computed through a smooth perturbation of the total energy curve with respect to the part's orientation angle θ, where θ is the measure of an angle with its initial side along the length direction of the binding site and its terminal side along the length direction of the part as shown in the inset of Figure 1(a). The values of surface energies γ between different solid surfaces are given as [31]

$$\gamma_{Si} = \gamma_{iA} - \gamma_{SA}\cos\varphi, \tag{9}$$

where γ_{Si} is the interfacial energy between the solder and the solid surface i. γ_{iA} is the surface energy between the solid surface i and the air environment, and γ_{SA} is the surface energy between the solder and the air environment. φ is the contact angle between the molten solder and the solid surfaces. In this investigation, solder, part, binding site and air environment are respectively denoted by S, P, B and A. The value of γ_{SA} can be measured by a goniometer. First, the total energy can be calculated for each orientation angle of the part. Then, the restoring torque τ acting on the part at different orientation angles is calculated based on the total energy curve.

Analysis

In this investigation, the magnet P has dimensions of $L_P \times W_P \times H_P = 18$ x 13 x 6 mm3, and the magnet Q has dimensions of $L_Q \times W_Q \times H_Q = 40$ x 10 x 7 mm3. The magnetizations of the magnets P and Q are $M_P \approx 9.71\times10^5$ A/m and $M_Q \approx 1.59\times10^5$ A/m, respectively. The magnets are magnetized along their longest dimension. The distance D and the distance Δ, indicated in Figure 1(a), are 8 mm and 10 mm, respectively. Figure 3(b) shows a B-H curve of an electroplated nickel part measured using a vibrating sample magnetometer (DMS-1660, ADE Technologies, USA). The rectangular part has a width of $W_{ni} = 5$ mm, a length of $L_{ni} = 10$ mm and a height $H_{ni} = 0.2$ mm. The number of minimum energy states depends on the width-to-length ratio of the rectangular parts. For solder self-assembly, the total interfacial energy is related to the overlap area between the part and the binding site.

The magnetic torque applied to the part is computed using (1-8). Figure 4 shows the magnetic torque as a function of the angle ranging from 0 to 180° between the length direction of the part and the magnet. The torque should have a periodicity of 180 degrees. The value of the magnetic torque is between -280 and 280 dyne·cm for one revolution of the magnet P. Due to geometric symmetry, the magnetic torque applied to the part with various orientation angles should lie in the range of -280 to 280 dyne·cm. The maximums of the magnitude of the magnetic torque lie at the orientation where the angle between the length direction of the magnet P and the part is 45°.

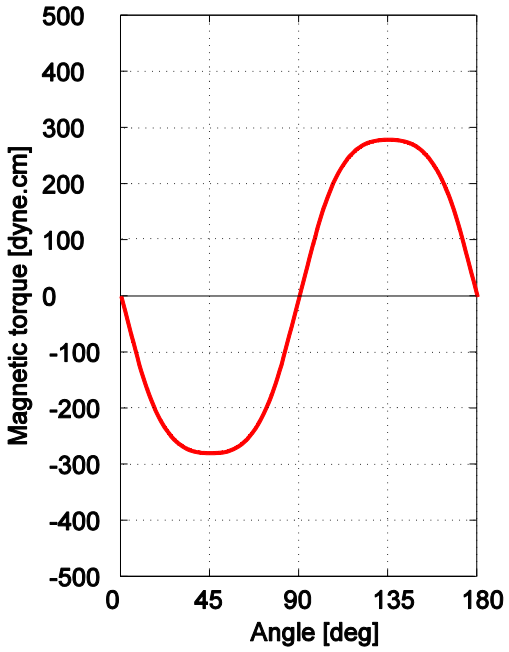

Figure 4. Magnetic torque as a function of the angle between the length direction of the part and the magnet.

Considering the self-assembly system without the magnets, the minimal energy surface is numerically calculated to predict the restoring torque applied to the part by the molten solder. It is assumed that the binding site has exactly the same lateral dimensions as the part. The binding site is wet with molten solder with a density of 9.7 g/cm^3 and a controlled volume of 0.1 cm^3. The value of γ_{SA} is measured as 503 dyne/cm. The values of surface energy between the air and the solid surfaces of nickel, γ_{PA}, and silica, γ_{BA}, are respectively taken as 1850 dyne/cm [32] and 300 dyne/cm [33]. The contact angles between the solder and the solid surfaces of the nickel and silica are respectively measured as 70° and 35°. The values of γ_{SP} and γ_{SB} are respectively calculated as 2206 and 49 dyne/cm by (9).

The Surface Evolver software is used to generate minimum-energy surfaces for part orientation angles ranging from 90° to 0° in incremental steps of 1°. The gravity for both the solder and the part is taken as 980 cm/sec^2, and the mass of the part is taken as 0.37 g in the

simulations. Restoring torques for different orientations are determined by the differentiation of the total energy with respect to the orientation angle. Figure 5 shows the total energy and restoring torque as functions of the part orientation angle. We obtained Figure 5 by calculating the total energy of the system at 91 orientation angles ranging from 0° to 90°. The differentiation of the total energy curve should be zero at 0° due to symmetry of the part and the solder geometry. The maximum of the total energy lies at the position of perfect alignment. The restoring torque has its maximum magnitude of 450 $\text{dyne}\cdot\text{cm}$ at the orientation near perfect alignment. The minimum magnitude of the restoring torque is 2.6 $\text{dyne}\cdot\text{cm}$ at $\theta = 90^{\circ}$. As the orientation angle decreases, the total energy increases. The positive initial slope indicates the assembly process for the part with an initial orientation angle between 0° and 90° is a nonspontaneous process. Leong et al. [17] pointed out that, as the size of the part increases, the weight increases and gravitational forces begin to dominate over the surface tension forces. Given proper design of parts, solder/liquid, binding sites and the fluidic/air environment, the self-assembly of micro and nano scale parts can be spontaneous. For the size of the part considered here, the external rotating magnetic field is needed for the nonspontaneous self-assembly process.

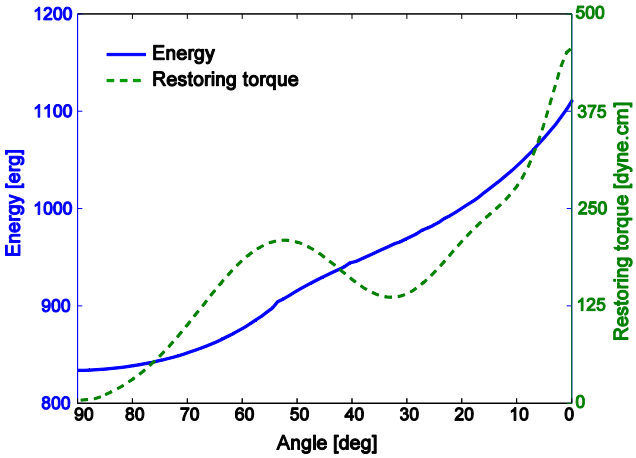

Figure 5. Total energy and restoring torque as functions of the orientation angle.

The results indicate that, for the selected magnetic properties and geometry of the part and magnets, the maximum magnitude of the magnetic torque is below the magnitude of the restoring torque when the part is in perfect alignment with the binding site. The misaligned part with various orientation angles can be agitated and rotated towards perfect alignment with the binding site, and stay in that orientation under the quasi-static condition. It is observed that the average angular velocity of the part rotated from $\theta = 90°$ towards $\theta = 0°$ is nearly 0.06 rad/sec, which is much smaller than the typical angular velocity of the rotating magnet, 25 rad/sec, used in the experiments. In this investigation, the misaligned part is rotated clockwise towards the perfect alignment given the clockwise rotation of the magnet. Compared to the much smaller angular velocity of the part, the rotating magnet serves to agitate the part and provides a clockwise moment to the part. Note that the inertial and damping effects due to the rotation of the part and the magnets are not considered in the analyses, which serve as a design guideline of the part and magnets used for this self-assembly method.

Experiments

A 5 X 10 mm2 rectangular pattern is cut out of a copper foil with a thickness 0.4 mm by milling. The patterned foil is then attached to a glass substrate to form a hydrophilic glass well in a hydrophobic copper surface. Electroplated nickel parts with dimensions of 5 X 10 X 0.2 mm3 are chosen in this investigation. Figure 6 shows a recessed hydrophilic well in a hydrophobic copper surface. Nickel parts are fabricated using a simple electroforming process. First, an electroplating tape is attached to a stainless steel substrate. A rectangular pattern is then cut out of the tape. Next, a 200 μm -thick nickel layer is electrodeposited using a low-stress nickel sulfamate bath. The electroplating tape is then detached from the substrate. Finally, the electroplated nickel layer is removed from the substrate by a thin slide. The fabricated part has a mass of 0.37 g.

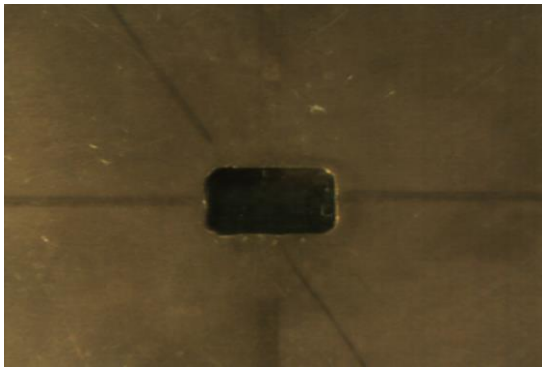

Figure 6. Patterned Cu layer on a substrate.

Solder is heated at 100° C until it is melted. The molten solder is then manually dropped into the binding site and wets only the hydrophilic binding site. After the coating process, only the hydrophilic binding site is coated with the molten solder. The amount of solder coated on the binding site is estimated as 0.1 cm^3. Figure 7 shows the experimental setup to demonstrate the self-assembly of the fabricated parts. A motor with a speed control unit is used to rotate the magnet P of NdFeB (Magtech Magnetic Products Co., Taiwan). The

magnet Q of ferrite (Taiwan Magnetic Co., Taiwan) is held by an acrylic fixture. A glass substrate containing the patterned copper foil is attached to a heating plate, which is heated at 80°C to keep the solder in a molten state.

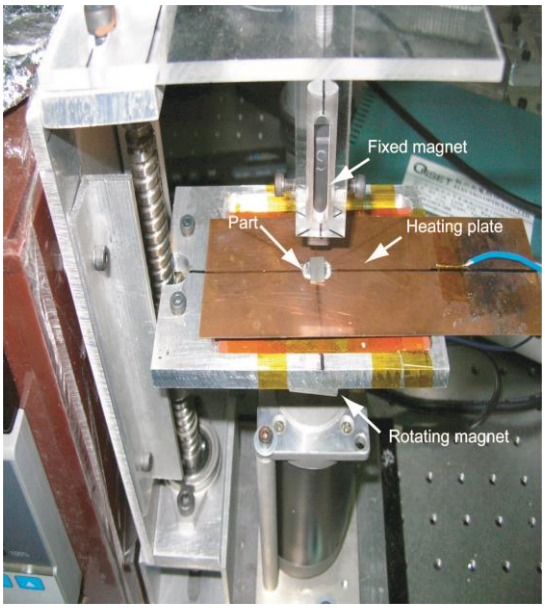

Figure 7. Experimental apparatus.

Results and Discussions

The angular velocity of the rotating magnet, Ω, for assembly of parts with orientation angles of 15°, 30°, 45°, 60°, 75° and 90° are 214 rpm, 264 rpm, 276 rpm, 280 rpm, 282 rpm, and 284 rpm, respectively. Figure 8 shows sequences of snapshots from experiments for $\theta = 45^\circ$. A high speed CCD camera (ST-EP130M-C, EPIX, Inc., US) is used to capture the successive images of the self-assembly process. The time for alignment of the parts is measured by the captured images. For a part with $\theta = 45^\circ$, the self-assembly is completed within 13.3 sec. Once alignment between parts and binding sites is achieved, the parts are kept aligned with the binding sites without oscillation. Figure 9 shows the time to alignment increases as the orientation angle θ increases.

One key point of assembly is to assemble large numbers of parts in a parallel and cost-effective manner. To demonstrate the parallel assembly capability of the proposed technique, experiments for six parts with orientation angles of 15°, 30°, 45°, 60°, 75° and 90° are carried out at room temperature in an air environment. Figure 10 (a) shows the six parts before assembly. Rectangular electroplated nickel parts measuring 3 X 6 X 1 mm^3 are chosen to demonstrate parallel assembly. Due to the large number of the parts employed in parallel assembly, the rectangular magnets used for the assembly of single parts are replaced with larger magnets. A cylindrical magnet with a radius of 15 mm, a height of 5 mm and magnetization of 159155 A/m is placed 2.7 cm above the glass substrate. A 50 X 20 X 10 mm3 rectangular magnet with a magnetization of 970845 A/m is placed 3.3 cm below the glass substrate. The magnet below the substrate provides magnetic torque.

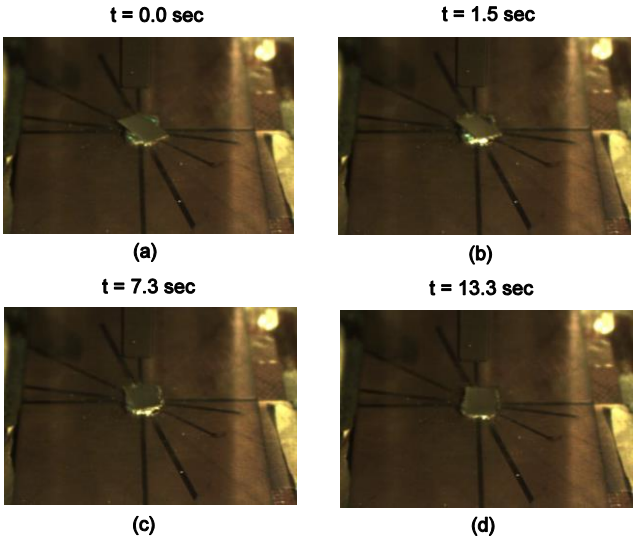

Figure 8. Snapshots of self-assembly of a part with an orientation angle of 45°.

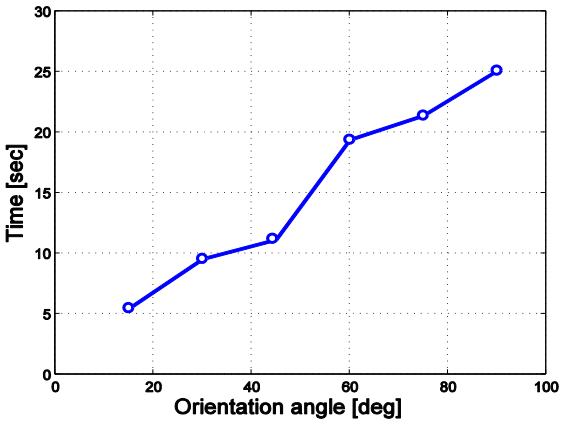

Figure 9. Alignment time with respect to various orientation angles.

During the assembly process, the temperature of the heating plate is set at $100^\circ C$. The angular velocity of the rotating magnet, Ω, is 300 rpm. Figure 10 (b) shows the parts aligned to the binding sites. The assembly is completed within 19 sec. During the experiments, once alignment between parts and binding sites is achieved, the parts maintain alignment without oscillation. The proposed method is designed to assemble large, millimeter-sized parts, where the alignment may require a combination of surface tension and other driving forces. As the weight or size of the parts decreases, surface tension begins to dominate and the self-assembly of the parts might be rendered spontaneous. The scalability of this technique needs further investigation.

(a) (b)

Figure 10. Parallel assembly of six parts.

The proposed assembling method using molten solder can be applied to integrate nanowires with a solder-padded substrate [22]. Another possible application is the assembly of two-dimensional structures to form three-dimensional solids [24]. It can also be used to assemble circular and square microparts to binding sites on a silicon template in a fluid environment [15], and to assemble square PZT parts in an air environment [18].

Conclusions

Magnetized millimeter-sized parts were self-assembled to the corresponding binding sites using molten solder and a rotating magnet. A theoretical model for predicting the magnetic torque to align parts was developed. The model can be used to determine the dimensions of the magnets and the parts for successful magnetic-assisted self-assembly. Batch assembly of six parts using an external magnetic field demonstrated the method can be implemented in a parallel and cost-effective manner, with batch assembly completed within 19 seconds with an orientation angle up to 135°. This approach, achieved without precise control of solder volume and complex robotic manipulation, is suitable for batch assembly of millimeter-sized, magnetized parts.

Acknowledgment

This work was financially supported by the National Science Council, Taiwan (Grant Number: NSC 96-2221-E-005-095). The authors would like to express their appreciation to members of the National Center for High-Performance Computing (NCHC), Taiwan for their assistance. Helpful discussions with Mr. Wen-Lin Chang of National Chung Hsing University are greatly appreciated.

References

[1] K. Mølhave, T. M. Hansen, D. N. Madsen, and P. Bøggild, "Towards pick-and-place assembly of nanostructures," *Journal of Nanoscience and Nanotechnology,* vol. 4, no. 3, pp. 279-282, 2004. doi: 10.1166/jnn.2004.025

[2] E. J. C. Bos, J. E. Bullema, F. L. M. Delbressine, P. H. J. Schellekens, and A. Dietzel, "A lightweight suction gripper for micro assembly," *Precision Engineering,* vol. 32, no. 2, pp. 100-105, 2008. doi: 10.1016/j.precisioneng.2007.05.003

[3] I. Giouroudi, H. Hötzendorfer, J. Kosel, D. Andrijasevic, and W. Brenner, "Development of a microgripping system for handling of microcomponents," *Precision Engineering,* vol. 32, no. 2, pp. 148-152, 2008. doi: 10.1016/j.precisioneng.2007.07.002

[4] A. S. Holmes and S. M. Saidam, "Sacrificial layer process with laser-driven release for batch assembly operations," *Journal of Microelectromechanical Systems,* vol. 7, no. 4, pp. 416-422, 1998. doi: 10.1109/84.735350

[5] A. Singh, D. A. Horsley, M. B. Cohn, A. P. Pisano, and R. T. Howe, "Batch transfer of microstructures using flip-chip solder bonding," *Microelectromechanical Systems, Journal of,* vol. 8, no. 1, pp. 27-33, 1999. doi: 10.1109/84.749399

[6] B. A. Grzybowski, M. Radkowski, C. J. Campbell, J. N. Lee, and G. M. Whitesides, "Self-assembling fluidic machines," *Applied Physics Letters,* vol. 84, no. 10, pp. 1798-1800, 2004. doi: 10.1063/1.1664019

[7] E. Saeedi, S. Abbasi, K. Böhringer, and B. A. Parviz, "Molten-alloy driven self-assembly for nano and micro scale system integration," *Fluid Dynamics & Materials Processing,* vol. 2, pp. 221-245, 2006. doi: 10.3970/fdmp.2006.002.221

[8] D. H. Gracias, J. Tien, T. L. Breen, C. Hsu, and G. M. Whitesides, "Forming electrical networks in three dimensions by self-assembly," *Science,* vol. 289, no. 5482, pp. 1170-1172, 2000. doi: 10.1126/science.289.5482.1170

[9] D. Sparks, G. Queen, R. Weston, G. Woodward, M. Putty, L. Jordan, S. Zarabadi, and K. Jayakar, "Wafer-to-wafer bonding of nonplanarized mems surfaces using solder," *Journal of Micromechanics & Microengineering,* vol. 11, no. 6, pp. 630-634, 2001. doi: 10.1088/0960-1317/11/6/303

[10] X. Xiong, Y. Hanein, J. Fang, Y. Wang, and D. T. S. a. K. F. B. W. WangT. Daniel, "Controlled multibatch self-assembly of microdevices," *Journal of Microelectromechanical Systems,* vol. 19, no. 8, pp. 117-127, 2003. doi: 10.1088/0960-1317/19/8/083001

[11] C. Videlot, J. Ackermann, F. Fages, T. N. Nguyen, L. Wang, P. M. Sarro, D. Crawley, K. Nikolić, and M. Forshaw, "Polymer interconnections for 3d-chip stacking technology: Directional volume patterning of flexible substrates with conducting polymer wires," *Journal of Micromechanics & Microengineering,* vol. 14, no. 12, pp. 1618-1684, 2004.
doi: 10.1088/0960-1317/14/12/004

[12] R. L. McCreery, "Molecular electronic junctions," *Chemistry of Materials,* vol. 16, no. 23, pp. 4477-4496, 2004.
doi: 10.1021/cm049517q

[13] J. Chung, Z. Wei, T. J. Hatch, and H. O. Jacobs, "Programmable reconfigurable self-assembly: Parallel heterogeneous integration of chip-scale components on planar and nonplanar surfaces," *Journal of Microelectromechanical Systems,* vol. 15, no. 3, pp. 457-464, 2006.
doi: 10.1109/JMEMS.2006.872226

[14] K. L. Scott, T. Hirano, H. Yang, H. Singh, R. T. Howe, and A. M. Niknejad, "High-performance inductors using capillary based fluidic self-assembly," *Journal of Microelectromechanical Systems,* vol. 13, no. 2, pp. 300-309, 2004.
doi: 10.1109/JMEMS.2003.823234

[15] C. J. Morris and B. A. Parviz, "Micro-scale metal contacts for capillary force-driven self-assembly," *Journal of Micromechanics & Microengineering,* vol. 18, no. 1, p. 015022, 2008.
doi: 10.1088/0960-1317/18/1/015022

[16] M. Liu, W. M. Lau, and J. Yang, "On-demand multi-batch self-assembly of hybrid mems by patterning solders of different melting points," *Journal of Micromechanics & Microengineering,* vol. 17, no. 11, pp. 2163-2168, 2007.
doi: 10.1088/0960-1317/17/11/001

[17] T. G. Leong, P. A. Lester, T. L. Koh, E. K. Call, and D. H. Gracias, "Surface tension-driven self-folding polyhedra," *Langmuir,* vol. 23, no. 17, pp. 8747-8751, 2007.
doi: 10.1021/la700913m

[18] J. Fang, K. Wang, and K. F. Böhringer, "Self-assembly of pzt actuators for micropumps with high process repeatability," *Journal of Microelectromechanical Systems,* vol. 15, no. 4, pp. 871-878, 2006.
doi: 10.1109/JMEMS.2006.878880

[19] K. F. Harsh, V. M. Bright, and Y. C. Lee, "Solder self-assembly for three-dimensional microelectromechanical systems," *Sensors and Actuators A: Physical,* vol. 77, no. 3, pp. 237-244, 1999.
doi: 10.1016/S0924-4247(99)00220-4

[20] H. O. Jacobs, A. R. Tao, A. Schwartz, D. H. Gracias, and G. M. Whitesides, "Fabrication of a cylindrical display by patterned assembly," *Science,* vol. 296, no. 5566, pp. 323-325, 2002.
doi: 10.1126/science.1069153

[21] S. A. Stauth and B. A. Parviz, "Self-assembled silicon networks on plastic," in *The 13th International Conference on Solid State Sensors Actuators (TRANSDUCERS)* 2005, vol. 1, pp. 964-967.
doi: 10.1109/SENSOR.2005.1496615

[22] H. Ye, Z. Gu, T. Yu, and D. H. Gracias, "Integrating nanowires with substrates using directed assembly and nanoscale soldering," *IEEE Transactions on Nanotechnology,* vol. 5, no. 1, pp. 62-66, 2006.
doi: 10.1109/TNANO.2005.861399

[23] K. Sato, K. Ito, S. Hata, and A. Shimokohbe, "Self-alignment of microparts using liquid surface tension-behavior of micropart and alignment characteristics," *Precision engineering,* vol. 27, no. 4, pp. 45-50, 2003.

[24] R. Gagler, A. Bugacov, B. E. Koel, and P. M. Will, "Voxels: Volume-enclosing microstructures," *Journal of Micromechanics & Microengineering,* vol. 18, no. 5, pp. 055025, 2008.
doi: 10.1088/0960-1317/18/5/055025

[25] B. A. Grzybowski, X. Jiang, H. A. Stone, and G. M. Whitesides, "Dynamic, self-assembled aggregates of magnetized, millimeter-sized objects rotating at the liquid-air interface: Macroscopic, two-dimensional classical artificial atoms and molecules," *Physical Review E,* vol. 64, pp. 011603, 2001.
doi: 10.1103/PhysRevE.64.011603

[26] J. J. Abbott, O. Ergeneman, M. P. Kummer, A. M. Hirt, and B. J. Nelson, "Modeling magnetic torque and force for controlled manipulation of soft-magnetic bodies," *IEEE Transactions on Robotics* vol. 23, no. 6, pp. 1247-1252, 2007.
doi: 10.1109/TRO.2007.910775

[27] R. I. Joseph and E. Schlömann, "Demagnetizing field in nonellipsoidal bodies," *Journal of Applied Physics,* vol. 36, no. 5, pp. 1579-1593, 1965.
doi: 10.1063/1.1703091

[28] J. Lienemann, A. Greiner, J. G. Korvink, X. Xiong, Y. Hanein, and K. F. Böhringer, "Modeling, simulation, and experimentation of a promising new packaging technology: Parallel fluidic self-assembly of microdevices," *Sensors Update,* vol. 13, no. 1, pp. 3-43, 2003.
doi: 10.1002/seup.200390012

[29] K. A. Brakke, "The surface evolver," *Experimental Mathematics,* vol. 1, pp. 141-165, 1992.

[30] K. A. Brakke, *Surface evolver manual*. Selinsgrove, PA, USA: Mathematics Department, Susquehanna University, 1999.

[31] T. Young, "An essay on the cohesion of fluids," *Philosophical Transactions of the Royal Society of London,* vol. 95, pp. 65-87, 1805. doi: 10.2307/107159

[32] G. A. Somorjai, *Introduction to surface chemistry and catalysis*. New York: J. Wiley & Sons, 1994.

[33] S. H. Ehrman, "Effect of particle size on rate of coalescence of silica nanoparticles," *Journal of Colloid and Interface Science,* vol. 213, no. 1, pp. 258-261, 1999. doi: 10.1006/jcis.1999.6105